AIAA JOURNAL
Vol. 34, No. 1, January 1996

Frequency-Load Interaction of Geometrically Imperfect Curved Panels Subjected to Heating

L. Librescu* and W. Lin†
Virginia Polytechnic Institute and State University, Blacksburg, Virginia 24061-0219
and
M. P. Nemeth‡ and J. H. Starnes Jr.§
NASA Langley Research Center, Hampton, Virginia 23681-0001

The results of a parametric study of the vibration behavior of flat and shallow curved panels subjected to temperature fields and mechanical loads are presented. The mechanical loads include uniform axial-compression prebuckling loads and transverse lateral pressure. The temperature fields include spatially nonuniform heating over the panel surfaces and a linear through-the-thickness temperature gradient. The structural analysis used for the study is based on a higher order transverse-shear-deformation shallow-shell theory that includes the effects of geometric nonlinearities and initial geometric imperfections. Analytical results are presented for simply supported single-layer and three-layer panels made from transversely isotropic materials. The results identify the interaction of the applied thermal and mechanical loads with the fundamental frequencies in both the prebuckling and postbuckling equilibrium states. The results indicate that initial geometric imperfections, transverse-shear flexibility, and changes in curvature are important contributors to the response of a panel for a wide range of structural and loading parameters.

Introduction

ADVANCED high-speed flight vehicles, such as a high-speed civil transport or an advanced tactical fighter, will experience high temperatures and pressure gradients during flight operations. These loading conditions typically occur in a dynamic environment. Major portions of the wing, fuselage, and empennage structures for these vehicles consist of flat and curved panels that are used as primary load carrying components. Changes in panel vibration characteristics due to the interaction of thermal and mechanical loads affect panel dynamic response and flutter characteristics. Thus, understanding the effects of thermal and mechanical loads on the response of vibrating flat and curved panels is necessary for determining and understanding the overall structural behavior of an aircraft.

Past studies of the vibration behavior of flat and curved panels subjected to elevated temperature fields have been limited in number, and most of these studies have focused on flat panels using classical plate theory (e.g., Refs. 1–6). The vibration behavior of infinitely long isotropic cylindrical panels subjected to thermal loads while in their prebuckling and postbuckling equilibrium states was investigated in Ref. 7. The comprehensive state-of-the-art reviews presented in Refs. 8 and 9, and the results presented in Ref. 10, have indicated the need for a better understanding of the effects of temperature fields, mechanical loads, and transverse-shear flexibility on the vibration characteristics of flat and curved panels in their prebuckling and postbuckling equilibrium states.

The present paper presents the results of an analytical study of the vibration behavior of single-layer and three-layer flat and shallow curved panels subjected to combined thermal and mechanical loads in their prebuckling and postbuckling equilibrium states. The panels are made of transversely isotropic materials, are symmetrically laminated, have uniform thickness, and are simply supported. The mechanical loads include uniform axial-compression prebuckling loads and lateral pressure. The thermal loads include both spatially nonuniform and linear through-the-thickness temperature fields. A special purpose analysis that is well suited for parametric studies and includes the effects of initial geometric imperfections and transverse-shear deformations is used for the present study. The results presented indicate the effects of thermal loads, combined thermal and axial-compression loads, lateral pressure, initial geometric imperfections, curvature, and transverse-shear flexibility on the vibration behavior of the panels. Results are presented for a wide range of loading and structural parameters.

Presented as Paper 94-1342 at the AIAA/ASME/ASCE/AHS/ASC 35th Structures, Structural Dynamics, and Materials Conference, Hilton Head, SC, April 18–20, 1994; received July 20, 1994; revision received July 23, 1995; accepted for publication Aug. 10, 1995.

*Professor, Department of Engineering Science and Mechanics.
†Graduate Student, Department of Engineering Science and Mechanics.
‡Senior Research Engineer, Structural Mechanics Branch. Senior Member AIAA.
§Head, Structural Mechanics Branch. Fellow AIAA.

Analysis Description

The analysis used in the present study is based on a higher order transverse-shear-deformation theory (HSDT) that includes the effects of geometric nonlinearities and initial geometric imperfections. A summary of the analysis is presented in the present paper, and details can be found in Refs. 10–15.

Thermoelastic Constitutive Relations

The thermoelastic constitutive equations used for the present study are for symmetrically laminated shallow curved panels with uniform thickness. The material is assumed to be elastic and transversely isotropic, with the plane of isotropy coinciding with the tangent plane at each point of the panel reference surface. The transversely isotropic constitutive equations are characterized by five elastic constants and two thermal coefficients: the elastic modulus E, Poisson's ratio ν, and the thermal compliance coefficient λ in the plane of material isotropy; and the elastic modulus E', Poisson's ratio ν', the shear modulus G', and the thermal compliance coefficient λ' perpendicular to the plane of isotropy. The coefficients of thermal expansion α and α' are related to the thermal compliance coefficients λ and λ' by equations presented in Refs. 14–16. For transversely isotropic materials, the transverse coefficient of thermal expansion α' is often much larger than the tangential coefficient of thermal expansion α. The transformed reduced thermoelastic constitutive equations used in the HSDT indicate that the thermal compliance coefficients depend on the ratio of the elastic moduli E/E'. The corresponding equations for classical shell theory do not depend

on this ratio. Also, the transformed reduced thermal compliance coefficients can be negative valued for ordinary values of E/E' and λ/λ' (see Ref. 17). These thermal compliance coefficients are always positive valued for a conventional isotropic material.

Nonlinear Boundary-Value Problem

The nonlinear equations used in the present study of the dynamic response of shallow curved panels are an extension of the classical von Kármán–Marguerre–Mushtari nonlinear shallow shell equations and include the effects of geometric imperfections and transverse-shear deformations. An Airy's stress function is used to eliminate the shell tangential-force equilibrium equations. The membrane-strain compatibility equation is included as a primary field equation of the nonlinear boundary-value problem along with the remaining shell transverse-force and moment equilibrium equations. A partially inverted form of the constitutive equations is used to express the membrane strains in terms of the Airy's stress function and the transverse displacement. The bending and transverse-shear-stress resultants are expressed in terms of the rotations and the transverse displacement. Substituting these special constitutive equations into the three remaining shell equilibrium equations and into the strain compatibility equation yields four coupled partial differential equations in terms of the stress function, the transverse displacement, and the two rotations. The equations are further reduced by expressing the rotations in terms of the transverse displacement and a potential function $\Gamma(x_1, x_2, t)$. Substituting the resulting expression into the out-of-plane force equilibrium equation yields an equation in terms of the stress function and the transverse displacement. Substituting this equation into the moment equilibrium equations yields a single Helmholtz type boundary-layer equation in Γ that is totally uncoupled from the other equations. In general, the boundary-value problem remains coupled through the five boundary conditions at each edge of the shell.

The panels considered in the present study have simply supported boundary conditions. The transverse displacement at each edge, the bending stress resultant acting about the axis parallel to each edge, and the rotation acting about the axis normal to each edge are all zero valued for these boundary conditions. The tangential displacements (in the tangent plane at each point of an edge) of the loaded and unloaded edges of a panel are unrestrained, and the edges are referred to herein as movable edges. The tangential stress resultants are specified at the edges.

For the simply supported boundary conditions considered, the nonlinear boundary-value problem is uncoupled with respect to the potential function Γ, and the solution to the Helmholtz type boundary-layer equation in Γ is $\Gamma = 0$. Thus, the nonlinear boundary-value problem reduces to two partial differential equations in terms of the Airy's stress function and the transverse deflection v_3 for both types of boundary conditions. These two equations are referred to herein as the von Kármán type compatibility equation and the transverse force equilibrium equation.

Solution of the Nonlinear Equations

The nonlinear boundary-value problem is solved using Galerkin's method. The transverse deflection v_3 is expressed in terms of functions that satisfy the simply supported boundary conditions

$$v_3(x_1, x_2, t) = w_{mn}(t) \sin \lambda_m x_1 \sin \mu_n x_2 \tag{1a}$$

where $\lambda_m = m\pi/L_1$, $\mu_n = n\pi/L_2$, and $w_{mn}(t)$ are the modal amplitudes and L_1 and L_2 are the panel side lengths. Following Ref. 18, the initial geometric imperfection $\overset{0}{v}_3$ is expressed as

$$\overset{0}{v}_3(x_1, x_2) = \overset{0}{w}_{mn} \sin \lambda_m x_1 \sin \mu_n x_2 \tag{1b}$$

where $\overset{0}{w}_{mn}$ are the modal amplitudes of the initial geometric imperfection shape. Similarly, the applied temperature and pressure fields are most generally represented by Navier type double Fourier sine series. In the present study, the temperature field is represented by

$$T(x_1, x_2, x_3) = \overset{0}{T}(x_1, x_2) + x_3 \overset{1}{T}(x_1, x_2) \tag{2a}$$

where

$$\overset{0}{T}(x_1, x_2) = \overset{0}{T}_{mn} \sin \lambda_m x_1 \sin \mu_n x_2 \tag{2b}$$

$$\overset{1}{T}(x_1, x_2) = \overset{1}{T}_{mn} \sin \lambda_m x_1 \sin \mu_n x_2 \tag{2c}$$

are expressed in terms of the temperature distributions at $x_3 = h/2$ and $-h/2$ where h is the panel thickness. The corresponding temperatures are denoted by T_i and T_e, respectively, and given by

$$\overset{0}{T} = \tfrac{1}{2}(T_i + T_e) \tag{2d}$$

$$\overset{1}{T} = (1/h)(T_i - T_e) \tag{2e}$$

Similarly, the pressure field is represented by

$$p_3(x_1, x_2) = p_{mn} \sin \lambda_m x_1 \sin \mu_n x_2 \tag{3}$$

The displacement expansions are substituted into the von Kármán type compatibility equation and the Airy's stress function is obtained by solving the resulting linear nonhomogeneous partial differential equation. The remaining nonlinear partial differential equation is the von Kármán type equilibrium equation that is converted into a set of nonlinear ordinary differential equations using Galerkin's method. This procedure yields the following set of $M \times N$ nonlinear ordinary differential equations for each set of wave forms determined by the index pair (m, n)

$$\begin{aligned} &A_{rs}\ddot{w}_{rs} + R_{rs}w_{rs} + p_{rs}B_{rs} - \Pi \overset{1}{T}_{rs}C_{rs} \\ &\quad + P_1\left[w_{rs}, \overset{0}{w}_{rs}, \tilde{L}_{11}, \tilde{L}_{22}\right] + P_2\left[w_{rs}^2, \overset{0}{w}_{rs}\right] + P_3\left[w_{rs}^3, \overset{0}{w}_{rs}\right] \\ &\quad + P_4\left[w_{rs}, \overset{0}{w}_{rs}, \overset{0}{T}_{rs}, \overset{1}{T}_{rs}\right] = 0 \end{aligned} \tag{4}$$

where the indices r and s are not summed and have the values $r = 1, 2, \ldots, M$ and $s = 1, 2, \ldots, N$. In Eq. (4), P_1 and P_4, P_2 and P_3 are linear, quadratic, and cubic polynomials of the unknown modal amplitudes $w_{rs}(t)$, respectively. The coefficients A_{rs}, B_{rs}, C_{rs}, and R_{rs} are constants that depend on the material and geometric properties of the panel or shell and $\tilde{L}_{11}$ and $\tilde{L}_{22}$ are normalized forms of the tangential stress resultants representing the mechanical loads.

Equations for Static Equilibrium States and Small Vibrations

The main emphasis of the present study is on the vibration behavior of flat and curved panels that are loaded quasistatically into their postbuckling load range. To obtain the equations that govern the static prebuckling and postbuckling equilibrium states, and the small vibrations about these equilibrium states, the unknown modal amplitudes are expressed as

$$w_{rs}(t) = \bar{w}_{rs} + \bar{\bar{w}}_{rs}(t) \tag{5}$$

The vibration amplitudes are considered small compared to $\bar{w}_{rs}$ and the imperfection amplitude $\overset{0}{w}_{rs}$ in the sense that

$$[\bar{\bar{w}}_{rs}(t)]^2 \ll \bar{w}_{rs}, \ \overset{0}{w}_{rs} \tag{6}$$

for all values of the indices r and s. The equations for the static prebuckling and postbuckling equilibrium states are obtained by discarding the inertia terms given by $A_{rs}\ddot{w}_{rs}$ in Eq. (4), and $\bar{w}_{rs}$ is the solution to the resulting equation. The equations for small vibrations about a given static equilibrium state are then obtained by substituting Eq. (5) into Eq. (4) and enforcing the smallness condition given by Eq. (6). The resulting equations of motion are given by

$$A_{rs}\ddot{\bar{\bar{w}}}_{rs}(t) + G_{rs}\bar{\bar{w}}_{rs}(t) = 0 \tag{7}$$

where

$$G_{rs} = G_{rs}\left(\bar{w}_{rs}, \bar{w}_{rs}^2, \bar{w}_{rs}^3, \overset{0}{w}_{rs}, p_{rs}, \overset{0}{T}_{rs}, \overset{1}{T}_{rs}\right) \tag{8}$$

for values of $r = 1, 2, \ldots, M$ and $s = 1, 2, \ldots, N$. The constant coefficients A_{rs} are functions of the material and geometric properties of the panel.

Small vibrations about a given equilibrium state are governed by Eq. (7), which is solved for synchronous motion by expressing $\bar{\tilde{w}}_{rs}(t)$ as

$$\bar{\tilde{w}}_{rs}(t) = \tilde{w}_{rs} e^{i\omega_{rs} t} \tag{9}$$

Substituting Eq. (9) into Eq. (7) yields an algebraic eigenvalue problem given by

$$G_{rs}\tilde{w}_{rs} = \omega_{rs}^2 A_{rs}\tilde{w}_{rs} \tag{10}$$

for values of $r = 1, 2, \ldots, M$ and $s = 1, 2, \ldots, N$. The frequencies ω_{rs} in Eq. (10) are the unknown quantities to be found, and the corresponding amplitudes $\tilde{w}_{rs}$ are indeterminate.

Response Characteristics and Computational Approach

The solution of Eq. (7) begins with the determination of the static equilibrium states for a flat or curved panel over a given range of a loading parameter. Two distinct types of thermal loading conditions are considered in the present study. The first type of thermal loading condition is associated with a temperature field that is uniformly distributed through the panel thickness, but nonuniformly distributed over the panel surfaces. This thermal loading condition generates membrane forces that can cause the panel to buckle. Flat panels have a stable postbuckling response with no reduction in load carrying capability at buckling, and the response is not sensitive to initial geometric imperfections. Curved panels have an unstable initial postbuckling response and their load carrying capability is reduced to a value that is less than the initial buckling load. The response of curved panels can be very sensitive to initial geometric imperfections. The second type of thermal loading condition is associated with a nonuniform through-the-thickness temperature distribution that is uniformly distributed over the panel surfaces. The through-the-thickness temperature gradient generates a thermal moment that causes the panel to bend. If the temperature gradient causes the panel to deflect so that it flattens as the temperature increases, the panel may have a limit-point instability response and may buckle or snap through to a secondary stable equilibrium state.

The static equilibrium configuration for a given flat or curved panel is obtained by solving the nonlinear algebraic equations given by Eq. (7) by using Newton's method. After determining the static equilibrium configuration of a panel for given values of the loading parameters, the coefficients A_{rs} and G_{rs} in Eq. (10) are computed, and the linear algebraic eigenvalue problem defined by Eq. (10) is solved. The solutions to these equations can be expressed in terms of the square of the fundamental frequency ω^2 and the applied thermal load. In general, Eq. (10) can have negative eigenvalues that correspond to pure imaginary fundamental vibration frequencies and unstable solutions that represent an unstable postbuckling equilibrium state.

Representative solutions for flat and curved panels with and without geometric imperfections and subjected to a thermal load that generates a membrane force P are indicated in Fig. 1. Solutions for panels with and without geometric imperfections are represented by the light and heavy lines, respectively. Solutions above the abscissa are physically admissible solutions that correspond to stable equilibrium states for the panels. Solutions below the abscissa are indicated by the shaded region in the figure, and are physically inadmissible solutions because they correspond to pure imaginary fundamental frequencies. The small arrows near the curves indicate the directions followed along the solution paths as the applied thermal load increases or decreases. As the applied thermal load increases from the origin of the figure for the panels without geometric imperfections, the fundamental frequencies decrease until the solutions intersect the abscissa. The fundamental frequencies are equal to zero on the abscissa, and the solutions change from a stable prebuckling equilibrium state by buckling or deforming into a stable postbuckling equilibrium state for the corresponding values of the thermal loads. After the panels have deformed into a stable postbuckling equilibrium state, additional increases in the applied thermal load

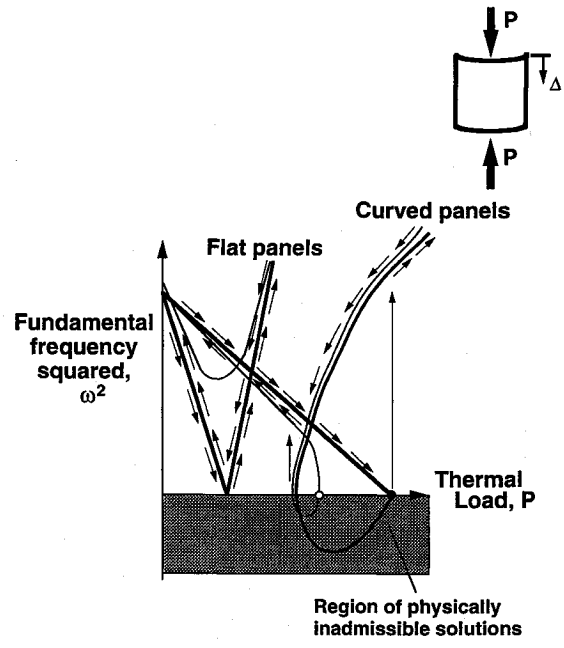

Fig. 1 Typical load-frequency responses curves for flat and curved panels with a uniform through-the-thickness temperature distribution: ——, geometrically perfect panels; and – – –, geometrically imperfect panels.

increase the fundamental frequencies. Decreasing the applied thermal load in a stable postbuckling equilibrium state decreases the fundamental frequencies until the solution path intersects the abscissa again, and the solutions change from the stable postbuckling equilibrium state to a stable prebuckling equilibrium state. Solutions that intersect the abscissa either buckle or have a limit-point instability response. Solutions that have a limit-point instability response do not entirely follow the same solution paths for increasing temperatures that they do for decreasing temperatures. Solutions that do not intersect the abscissa change from one stable equilibrium state to another and may have a limit-point instability response. The solutions for the flat panels with geometric imperfections do not intersect the abscissa, and these solutions are always stable. Solutions for the curved panels with geometric imperfections respond similarly to the curved panels without geometric imperfections, but the transition from one stable equilibrium state to another occurs at a lower value of the applied thermal load.

Results and Discussion

A comparison of results from the present study with corresponding available analytical and experimental results presented in Ref. 19 is shown in Fig. 2. The load-frequency response results in Fig. 2 relate the frequency ratio $(\omega/\Omega)^2$ and the load ratio $N_{11}/(N_{11})_{cr}$ for a geometrically imperfect rectangular flat metallic panel where Ω is the fundamental frequency of the unloaded panel and $(N_{11})_{cr}$ is the value of N_{11} at buckling. The results presented in Fig. 2 agree very well, which indicates that the present analysis represents the response of these flat panels very well. Although not shown in the present paper, the present results and the analytical results presented in Refs. 20–22 for both perfect and geometrically imperfect panels also agree very well. The corresponding results for curved panels do not appear to be available in the open literature.

The results presented in the present paper are for simply supported flat and curved panels with movable edges. The panels have a square planform with side length dimensions $L_1 = L_2 = \ell$ and consist of either a single layer or three layers of transversely isotropic elastic material. The values of the Poisson's ratios and the coefficient of thermal expansion used for the analyses are $\nu = \nu' = 0.2$ and $\alpha = 1.15 \times 10^{-6}$ in./in./°F (2.07×10^{-6} mm/mm/°C), respectively. The elastic moduli and coefficients of thermal expansion for the single-layer panels are expressed as constant nondimensional ratios with values of $E'/E = 5$ and $\alpha'/\alpha = 15$, respectively. The shear modulus G' is expressed as a ratio of the elastic modulus to the shear

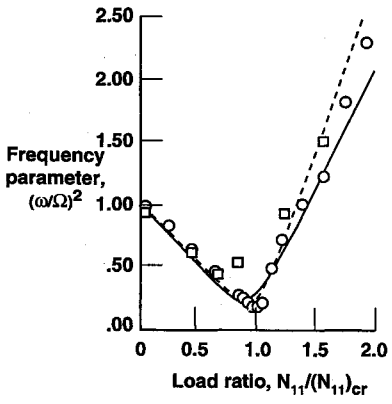

Fig. 2 Comparison of analytical and experimental results from Ref. 19 with results from the present analysis: ——, analysis, present study; ---, analysis[19]; o, experiments (loading)[19]; and □, experiments (unloading).[19]

modulus E/G' and a value of $E/G' = 30$ is used for panels with a moderate degree of transverse-shear flexibility, unless otherwise noted. The ratio of E/G' is varied for some of the single-layer panels to determine the effects of transverse-shear flexibility on the results. The properties of the outer layers of the three-layer panels are the same as for the single-layer panels, and the inner layer is twice as thick as an outer layer. The elastic moduli and thermal compliance coefficients for the outer layers are constant nondimensional ratios with values of $(E'/E)_f = 5$, $(E/G')_f = 10$, and $(\lambda/\lambda')_f = 1.43$, respectively, where the subscript f indicates the outer layers. Similarly, the elastic moduli and thermal compliance coefficients for the inner layer are constant nondimensional ratios with values of $(E'/E)_c = 2$, $(E/G')_c = 30$, and $(\lambda/\lambda')_c = 1.21$, respectively, where the subscript c indicates the inner layer. The temperature field is specified to be a sinusoidal function distributed across each surface of the panels considered [see Eqs. (2a–2c)]. Two through-the-thickness temperature distributions are considered in this study. One temperature distribution has the same value of temperature on both panel surfaces ($T_i = T_e$), and the other temperature distribution has unequal values of temperature on the panel surfaces ($T_i \neq T_e$). A constant temperature value of $T_e = 70°\text{F}\ (21°\text{C})$ at $x_1 = x_2 = \ell/2$ is used for all results presented with a through-the-thickness temperature gradient, unless otherwise noted.

Most of the results are presented in the form of interaction curves that relate the magnitude of the average middle surface temperature $\overset{0}{T}_{mn}$ to the square of the fundamental frequency as a function of the axial-compression prebuckling load, the geometric imperfection amplitude, and the degree of transverse-shear flexibility. The square of the fundamental frequency ω^2, the applied inplane compression load N_{11}, and the applied transverse pressure load p_3 are represented in the figures by the following nondimensional parameters:

$$\bar{\omega}^2 = \frac{\omega^2 m_0 \ell^4}{\pi^4 D} \tag{11a}$$

$$\tilde{L}_{11} = \frac{N_{11}\ell^2}{\pi^4 D} \tag{11b}$$

$$p_0 = \frac{p_3(\ell/2, \ell/2)\ell^4}{Dh} \tag{11c}$$

where m_0 is the reduced mass and $D = Eh^3/12(1-\nu^2)$ is the isotropic panel bending stiffness. At buckling, the parameter $\tilde{L}_{11}$ corresponds to the well-known definition of the buckling coefficient for isotropic panels. This coefficient has a value of 4 for the simply supported, square flat panels considered herein. A nondimensional initial geometric imperfection amplitude $\delta_0 = \overset{0}{v}_3(\ell/2, \ell/2)/h$ is also used in the figures.

Results for flat panels are presented in Figs. 3–5, and results for curved panels are presented in Figs. 6–8. Results are also presented in Fig. 9 that show a comparison between results obtained using different shell theories to account for transverse-shear flexibility. The fundamental frequencies for both the prebuckling and postbuckling equilibrium states correspond to mode shapes given by $m = n = 1$ for the range of structural parameters considered and for all of the results presented herein. The maximum values of the temperature and pressure are given by the temperature $\overset{0}{T}_{11}$ and pressure p_{11} at $x_1 = x_2 = \ell/2$ and are denoted for convenience by $\overset{0}{T}$ and p_3, respectively. A similar convention is applied to T_e and T_i, which in the numerical applications denote the temperature amplitudes at the center of the upper and bottom faces, respectively.

Results for Flat Panels

The effects of a uniform through-the-thickness temperature increase ($T_i = T_e$) and an axial-compression prebuckling load on the fundamental vibration frequency of thin, geometrically perfect, single-layer panels with $\ell/h = 60$ are shown in Fig. 3a for six values of the nondime2nsional prebuckling load $\tilde{L}_{11}$ ranging from 0 to 2.5. These panels have perfectly flat prebuckling shapes and buckle at the bifurcation points indicated by the filled circles on the abscissa due to the nonuniform temperature distribution over the panel top and bottom surfaces. The results indicate that the fundamental frequency decreases linearly as the thermal load increases prior to buckling for a given mechanical prebuckling load. The fundamental frequency also decreases as the mechanical prebuckling load increases in the prebuckling load range. Increasing the thermal load or the applied mechanical prebuckling load increases the in-plane compression load in the panel that reduces the frequency due to the additional bending moment caused by the nonlinear coupling of the in-plane load with the out-of-plane displacements. At buckling, the fundamental frequency is zero valued as indicated by the filled circles in the figure. The highest buckling temperature is predicted for the panels without a mechanical prebuckling load, and the buckling temperature decreases as the magnitude of the mechanical prebuckling load increases. The fundamental frequency increases as the temperature increases above the buckling temperature, and panels with lower values of mechanical prebuckling load have lower fundamental frequencies for a given temperature level. The increase in fundamental frequency for temperatures above the buckling temperature is attributed to the change in the panel geometry that occurs after buckling. When a flat panel buckles, it buckles into a buckling mode shape that is a curved surface. The curvature of the buckled panel increases the panel bending stiffness, which increases the panel fundamental frequency.

The effects of a through-the-thickness temperature gradient ($T_i \neq T_e$) and a mechanical prebuckling load on the fundamental frequency of thin single-layer panels with $\ell/h = 60$ are shown in Fig. 3b for the same six nondimensional prebuckling loads $\tilde{L}_{11}$ as for Fig. 3a. The through-the-thickness temperature gradient corresponds to a surface temperature amplitude $T_e = 70°\text{F}\ (21°\text{C})$ and the temperature T_i given by Eq. (2c) for specified values of $\overset{0}{T}$ or $T_i = 2\overset{0}{T} - T_e$. The applied temperature gradient generates an in-plane compression load in the panel and a bending moment that causes out-of-plane deflections. The panels do not have a bifurcation buckling load because the out-of-plane deflections occur from the onset of the applied loads. The applied mechanical prebuckling load generates an additional bending moment caused by the coupling of the in-plane load with the out-of-plane displacements. The results indicate similar general trends for the interaction curves relating the applied thermal gradient and the fundamental frequency as those for the uniform through-the-thickness temperature shown in Fig. 3a. The fundamental frequency decreases monotonically as the magnitude of the thermal gradient increases and then increases monotonically for values of $\overset{0}{T}$ greater than the temperature corresponding to the minimum frequency for each curve. This change in response is attributed to the nonlinear coupling of the in-plane forces with the out-of-plane deflections and the bending moments that occur as $\overset{0}{T}$ is increased from a value of zero. The increase in fundamental frequency is due to increases in panel stiffness as the deflections become large enough to generate curvature in the panel. Increasing the mechanical prebuckling load decreases the fundamental frequency for the smaller values of $\overset{0}{T}$, and increases the fundamental frequency for the larger values. This trend suggests that an increase in the magnitude of the compressive prebuckling load amplifies the magnitude of the out-of-plane deflections.

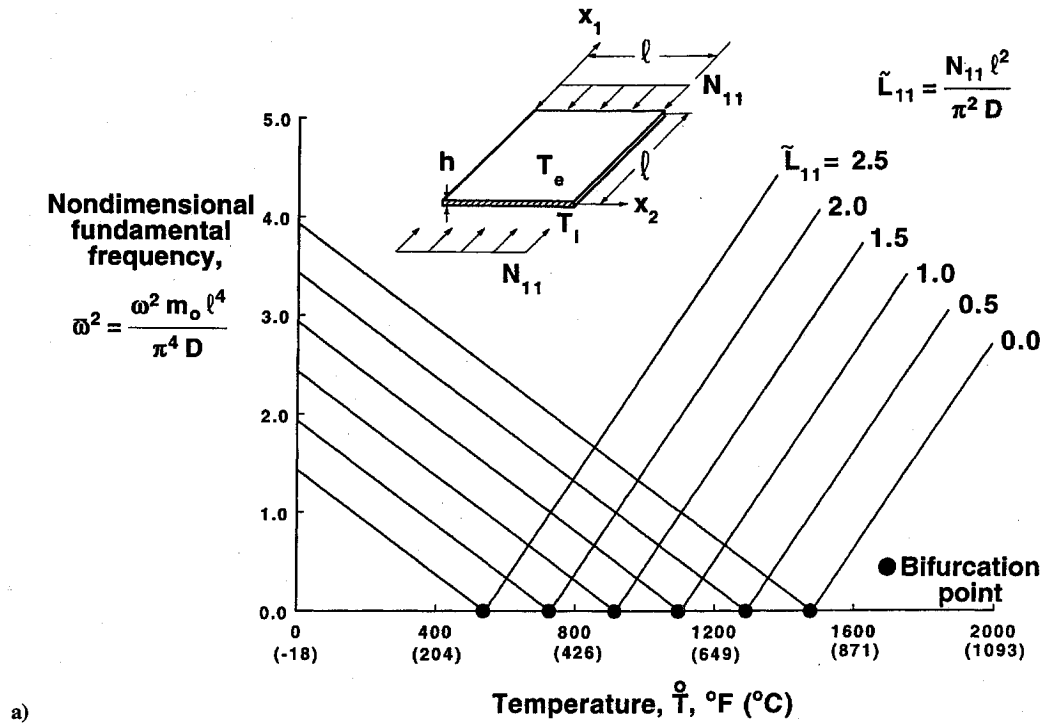

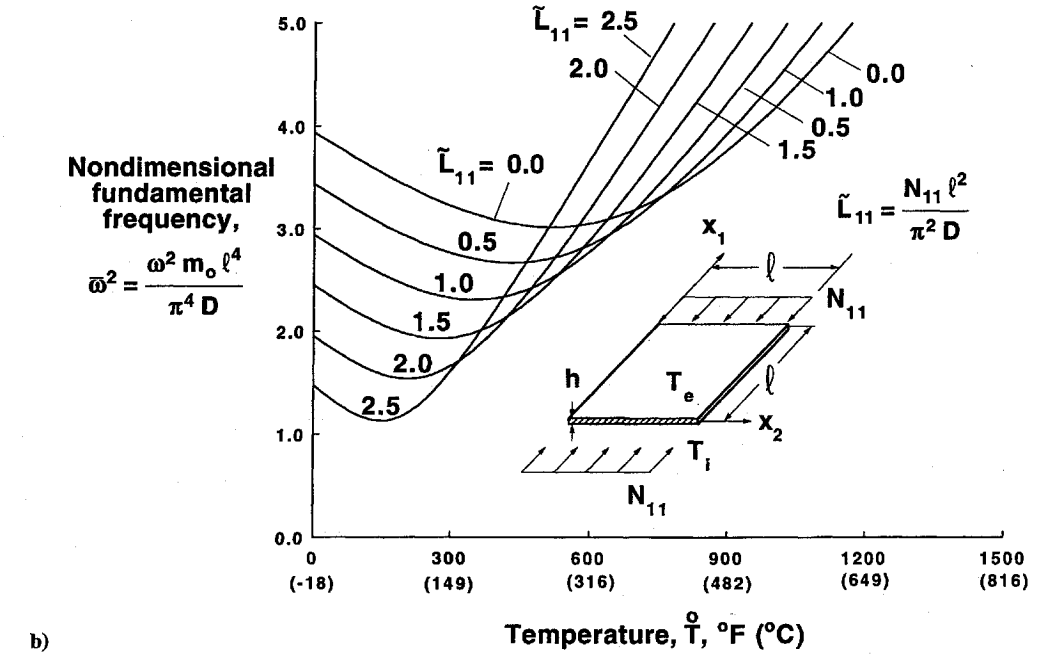

Fig. 3 Effects of uniform axial-compression mechanical prebuckling loads and temperature increase on the fundamental frequency of single-layer flat panels: a) uniform through-the-thickness temperature increase and b) through-the-thickness temperature gradient with T_e = 70°F (21°C).

The effects of transverse-shear flexibility on the interaction curves relating an applied uniform through-the-thickness temperature ($T_i = T_e$) and the fundamental frequency of single-layer panels with $\ell/h = 30$ are shown in Fig. 4a for axial-compression prebuckling loads that are 75% of corresponding panel buckling loads. Results are presented for values of $E/G' = 0$, 10, 30, and 50. The results for $E/G' = 0$ correspond to results from classical plate theory. The results for a given value of temperature indicate that an increase in transverse-shear flexibility causes a significant decrease in fundamental frequency in the prebuckling temperature range and an increase in frequency in the postbuckling temperature range. An increase in transverse-shear flexibility causes larger out-of-plane vibration deflections in the prebuckling temperature range that correspond to a more flexible panel with a lower fundamental frequency. The temperature–frequency interaction trend changes in the postbuckling temperature range where the frequency increases as the temperature increases. The increase in transverse-shear flexibility causes larger out-of-plane deflections in the postbuckling temperature range that increase the curvature and overall bending stiffness of the panel and, as a result, increase the fundamental frequency.

The effects of transverse-shear flexibility on the interaction curves relating an applied through-the-thickness temperature gradient ($T_i \neq T_e$) with T_e = 70°F (21°C) and the fundamental frequency of single-layer panels with $\ell/h = 30$ are shown in Fig. 4b for the same mechanical prebuckling loads as Fig. 4a. The results indicate that an increase in transverse-shear flexibility generally decreases the fundamental frequency up to a value of T of approximately 450°F (232°C) where the curve for $E/G' = 50$ intersects the curve for $E/G' = 30$ and has a higher frequency for

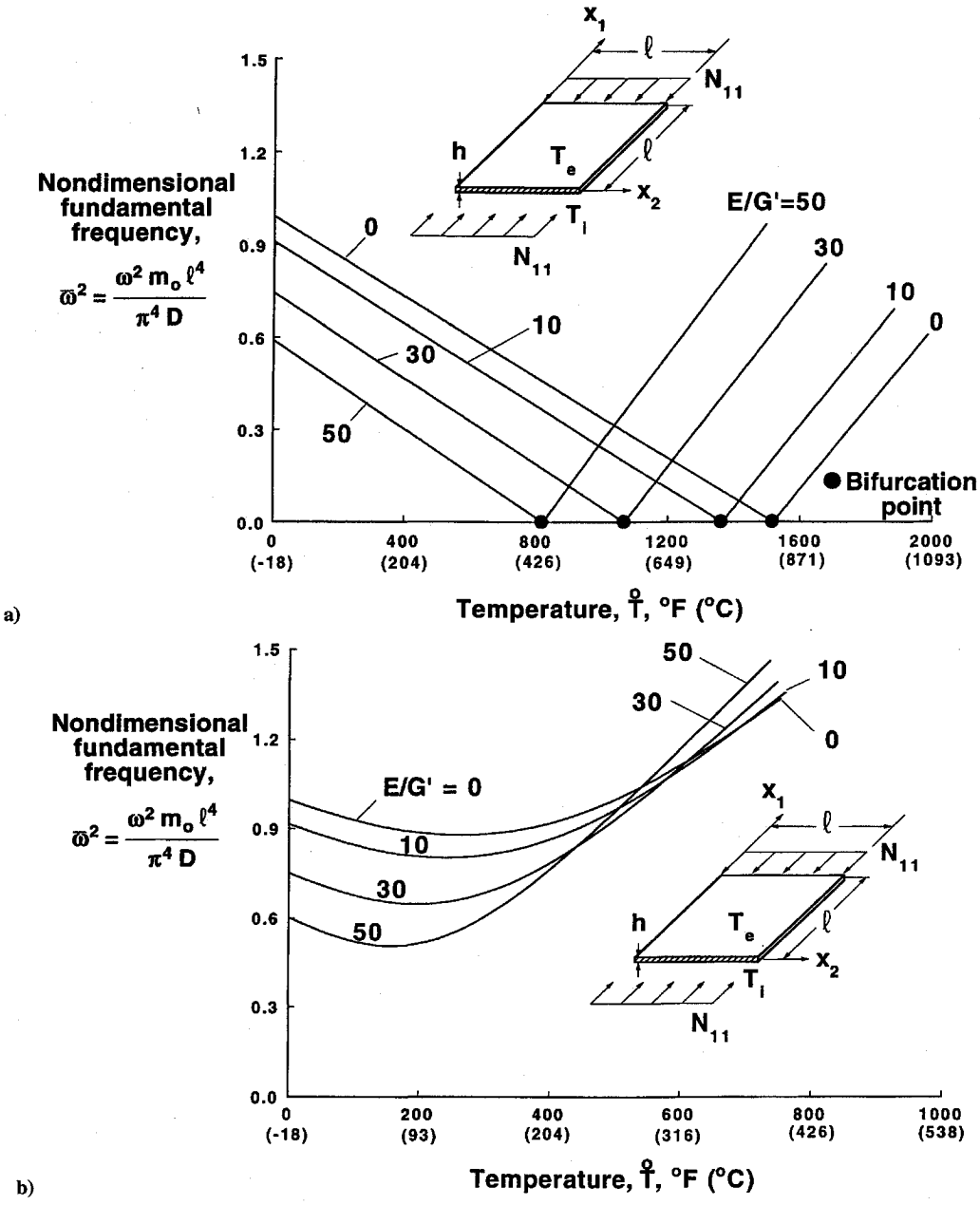

Fig. 4 Effects of transverse-shear flexibility E/G' on the fundamental frequency of flat single-layer panels subjected to a mechanical prebuckling load that is 75% of the corresponding buckling load and to a temperature increase: a) uniform through-the-thickness temperature increase and b) through-the-thickness temperature radient with T_e = 70°F (21°C).

larger values of temperature. The sensitivity of the fundamental frequency to increases in transverse-shear flexibility decreases as the temperature gradient increases.

The effects of initial geometric imperfections and panel thickness on the interaction curves relating an applied uniform through-the-thickness temperature ($T_i = T_e$) and the fundamental frequency of single-layer panels with a moderate value of transverse-shear flexibility ($E/G' = 30$) are shown in Fig. 5a. Results for a panel length-to-thickness ratio of $\ell/h = 60$ are indicated by the dashed lines and results for $\ell/h = 100$ are indicated by the solid lines for three different imperfection amplitudes given by $\delta_0 = \overset{0}{v}_3(\ell/2, \ell/2)/h = 0.0, 0.2$, and 0.4. The imperfection shape is a half-sine wave along each coordinate direction. The results shown in the figure for $\delta_0 = 0.0$ have bifurcation buckling loads indicated by the filled circles on the abscissa, which is consistent with the behavior of flat panels without imperfections. The results indicate that the thicker panels have higher buckling temperatures. The fundamental frequencies increase as the imperfection amplitude increases for both the prebuckling and postbuckling temperature ranges and for both length-to-thickness ratios. The thinner panels have lower fundamental frequencies in the prebuckling temperature range and higher frequencies in the postbuckling temperature range and are typically more sensitive to increases in imperfection amplitude than the corresponding thicker panels.

The effects of initial imperfections and panel thickness on the interaction curves relating an applied through-the-thickness temperature gradient ($T_i \neq T_e$) with T_e = 70°F (21°C) and the fundamental frequency of single-layer panels with a moderate value of transverse-shear flexibility ($E/G' = 30$) are shown in Fig. 5b for the same values of ℓ/h and δ_0 as for Fig. 5a. The results indicate that the fundamental frequencies increase as the imperfection amplitude increases and that the thinner panels are typically more sensitive to increases in imperfection amplitude than the thicker ones.

Results for Curved Panels

The effects of panel curvature on the interaction curves relating an applied uniform through-the-thickness temperature ($T_i = T_e$) and the fundamental frequency of three-layer cylindrical panels with $\ell/h = 60$ are shown in Fig. 6a for values of ℓ/R_2 ranging from 0.0 to

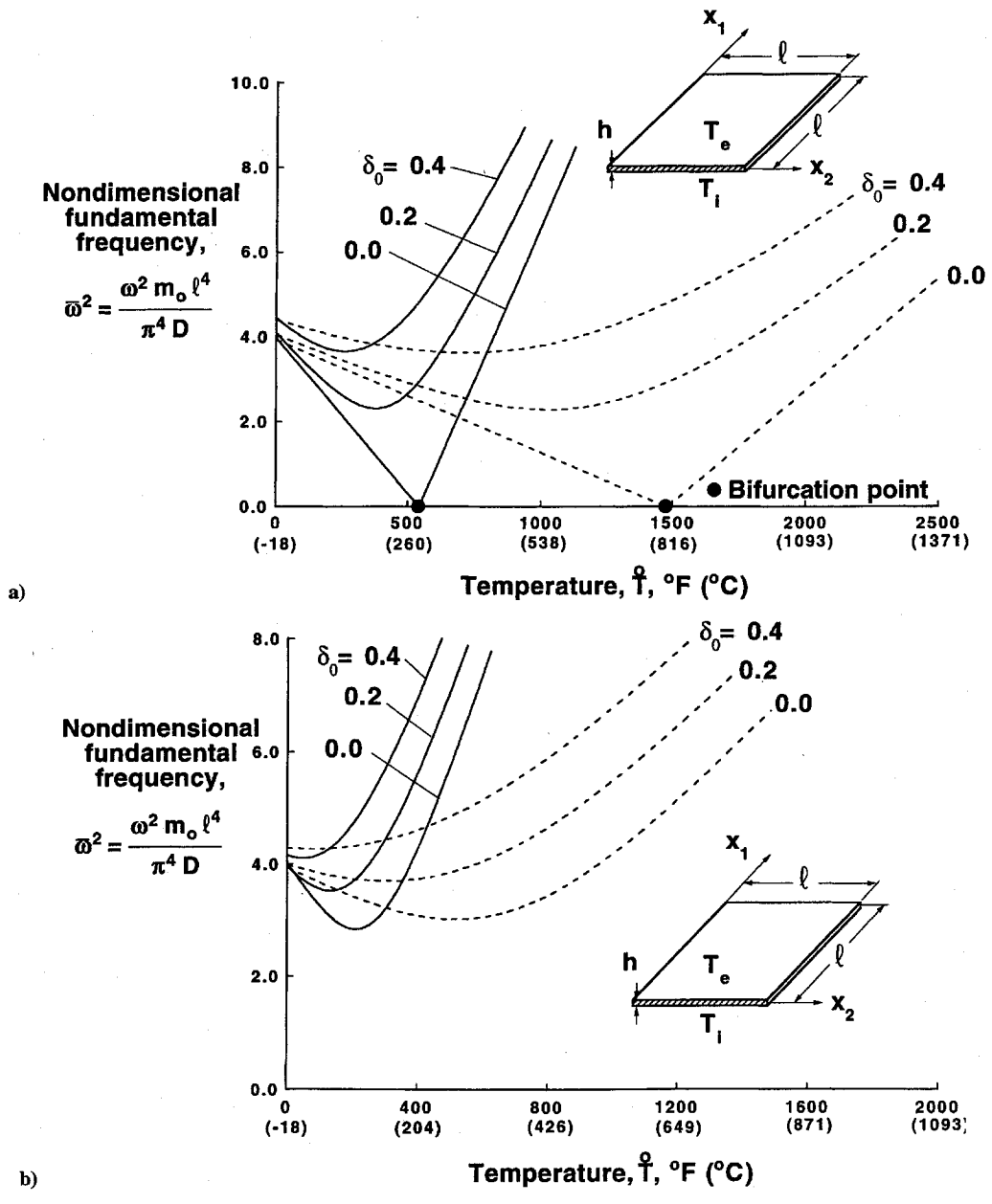

Fig. 5 Effects of initial geometric imperfections, plate length-to-thickness ratio, and temperature increase on the fundamental frequency of single-layer flat panels: a) uniform through-the-thickness temperature increase and b) through-the-thickness temperature gradient with T_e = 70°F (21°C).

0.3, where $\ell/R_2 = 0.0$ corresponds to a flat panel. The limiting case of a flat panel has a stable bifurcation buckling response as indicated by the filled circle on the abscissa. Increasing the panel curvature increases the fundamental frequency without causing a limit-point instability response as the temperature increases. The convex surface of a curved panel has a larger radius than the concave surface and, as a result, has a larger circumferential thermal expansion than the concave surface for an increase in a uniform through-the-thickness temperature. This difference in circumferential thermal expansions increases the panel curvature, and as a result, increases the panel bending stiffness, which increases the fundamental frequency.

The effects of panel curvature on the interaction curves relating an applied through-the-thickness temperature gradient ($T_i \neq T_e$) and the fundamental frequency of three-layer cylindrical panels with $\ell/h = 60$ are shown in Figs. 6b and 6c for values of ℓ/R_2 ranging from 0.0 to 0.3, where $\ell/R_2 = 0.0$ corresponds to a flat panel. The results presented in Fig. 6b are for temperature gradients with a constant concave-surface-temperature value of $T_i = 70°F(21°C)$, and the temperature T_e is given by Eq. (2c) for the specified values of $\overset{\circ}{T}$. The results indicate a general monotonically increasing trend of the fundamental frequency as the temperature of the convex surface increases. Increasing the panel curvature increases the fundamental frequency as the temperature increases without causing a limit-point instability response. This response suggests that the convex surface deforms away from its projected planform ($x_3 = 0$) into a surface with an increased positive Gaussian curvature as its temperature increases. This increase in curvature increases the panel bending stiffness, which increases the fundamental frequency.

The results presented in Fig. 6c are for temperature gradients with a constant convex-surface-temperature value of $T_e = 70°F(21°C)$, and the temperature T_i is given by Eq. (2c) for the specified values of $\overset{\circ}{T}$. These results indicate that a much more complex interaction occurs between the thermal load and the fundamental frequency as the temperature of the concave surface increases. For $\overset{\circ}{T} = 0$ the concave surface temperature is $T_i = -70°F(-57°C)$, and the flat panel deflects in the negative x_3 direction and deforms into a surface with a positive Gaussian curvature. As the magnitude of the temperature gradient increases, this deformed surface tends to flatten and subsequently deforms in the positive x_3 direction. As the deformed surface flattens, the fundamental frequency decreases because the panel bending stiffness decreases. As the deformed surface begins to develop more curvature, the fundamental frequency increases

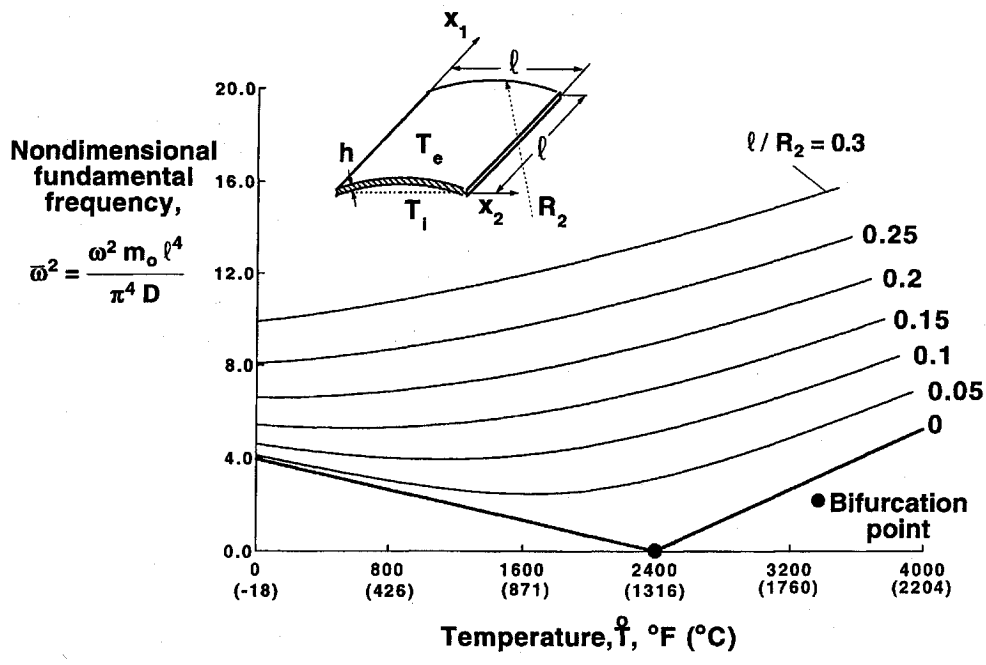

a)

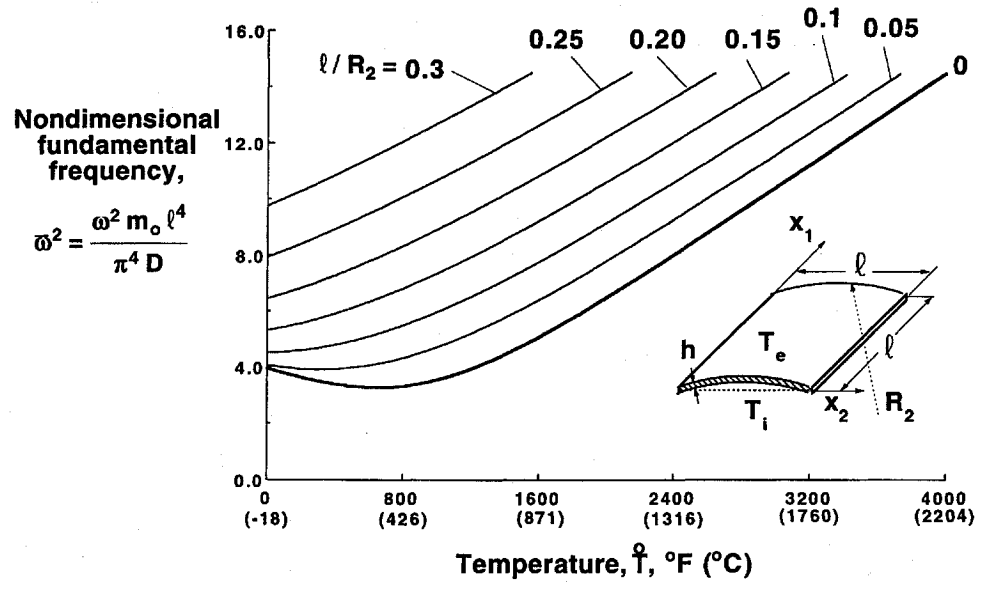

b)

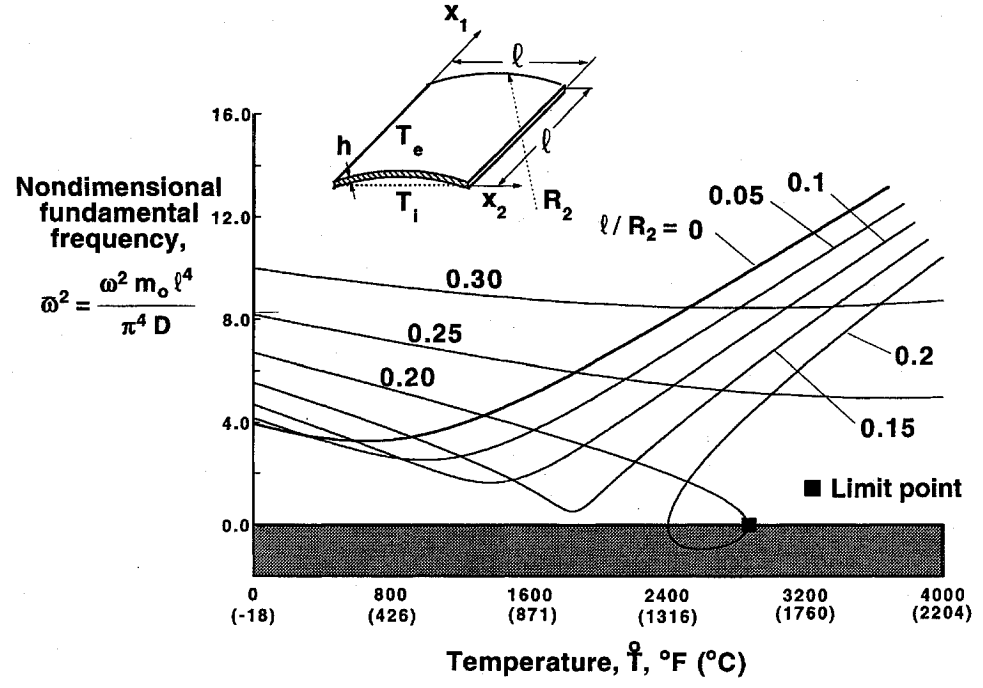

c)

Fig. 6 Effects of curvature on the fundamental frequency of three-layer cylindrical panels subjected to a temperature increase: a) uniform through-the-thickness temperature increase, b) through-the-thickness temperature gradient with T_i = 70°F (21°C), and c) through-the-thickness temperature gradient with T_e = 70°F (21°C).

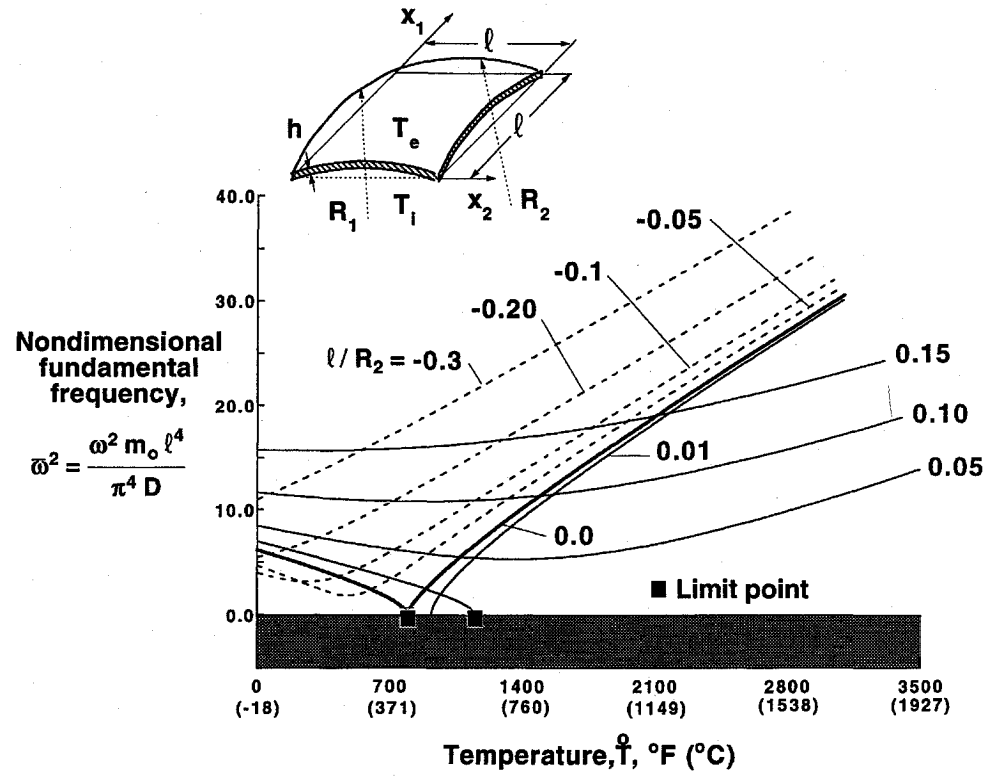

a)

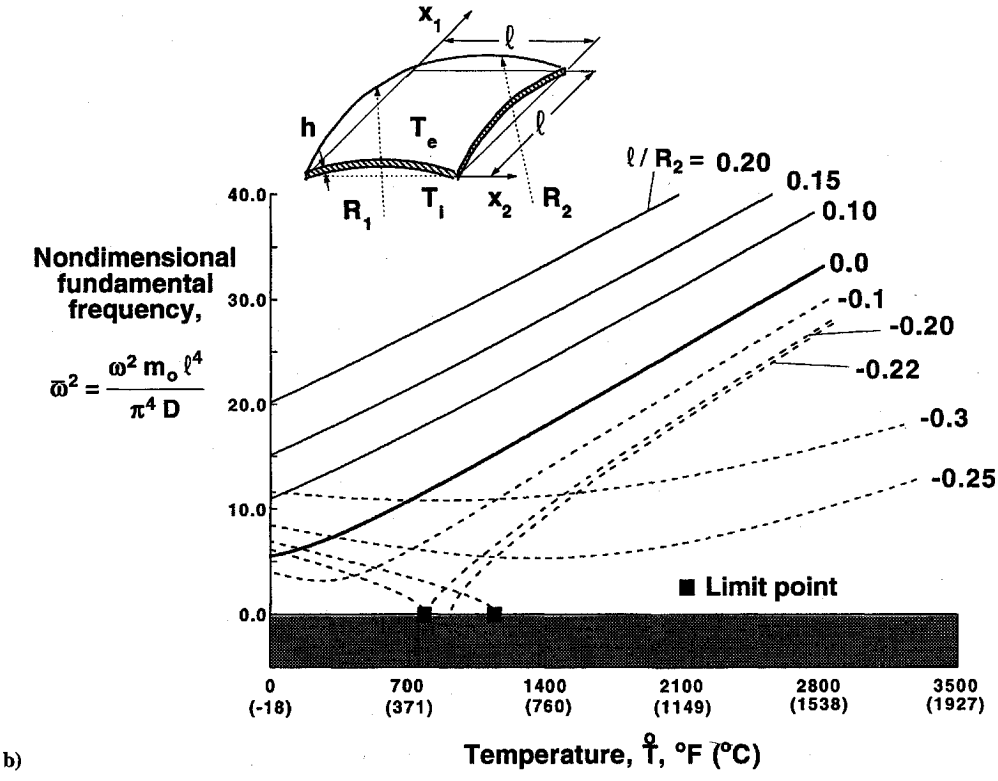

b)

Fig. 7 Effect of compound curvature on the fundamental frequency of three-layer flat doubly curved panels subjected to a nonuniform through-the-thickness temperature increase and with $\ell/R_1 = 0.1$: - - - -, negative Gaussian curvature; ——, positive Gaussian curvature: a) through-the-thickness temperature gradient with $T_e = 70°F$ (21°C); and b) through-the-thickness temperature gradient with $T_i = 70°F$ (21°C).

because the panel bending stiffness increases. The curved panels generally behave in a similar manner since the curvature of the deformed configurations for $\overset{0}{T} = 0$ have increased, which increases the panel bending stiffness and, as a result, increases the fundamental frequency. As ℓ/R_2 increases, the panels become susceptible to a limit-point instability response as indicated by the filled square on the abscissa for the panel with $\ell/R_2 = 0.2$, and the panels buckle or snap through into another stable equilibrium state. As ℓ/R_2 increases beyond 0.2, the panels are no longer susceptible to a limit-point instability response, and an increase in temperature decreases the curvature of the deformed panel, which decreases the fundamental frequency monotonically.

The effects of compound panel curvature on the interaction curves relating an applied through-the-thickness temperature gradient ($T_i \neq T_e$) and the fundamental frequency of thin three-layer panels with $\ell/h = 100$ are shown in Figs. 7a and 7b for several positive and negative values of ℓ/R_2 and a constant value of $\ell/R_1 = 0.1$. The heavy solid lines in the figures correspond to a cylindrical panel with

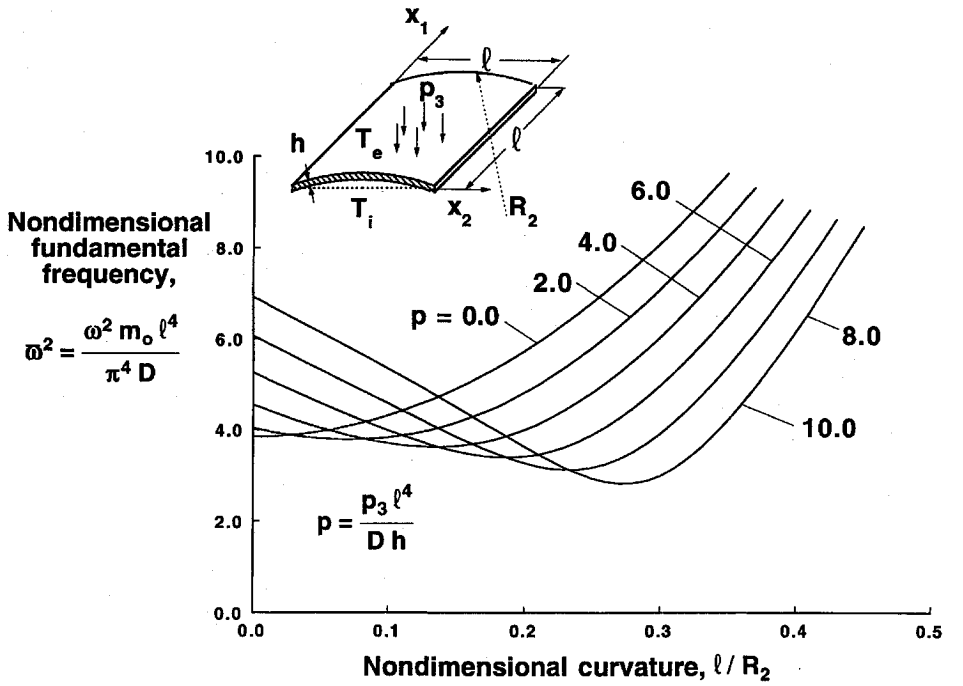

Fig. 8 Effects of an external lateral pressure load and curvature on the fundamental frequency of single-layer cylindrical panels subjected to a uniform through-the-thickness temperature.

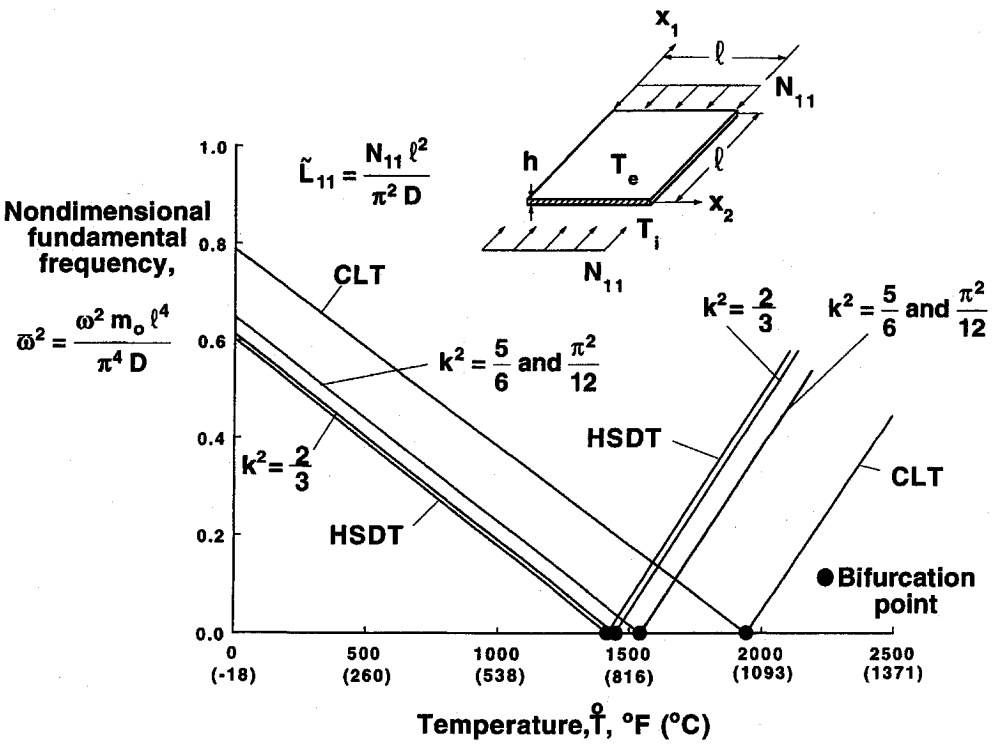

Fig. 9 Comparison of results obtained for three-layer flat panels using HSDT with results for CLT and FSDT.

$\ell/R_2 = 0.0$ and zero Gaussian curvature. The lighter solid lines and dashed lines correspond to results for doubly curved panels with positive and negative Gaussian curvature, respectively. The results presented in Fig. 7a are for the case in where the convex surface temperature remains constant at $T_e = 70°F(21°C)$ and the concave surface temperature increases. The results presented in Fig. 7b are for the case where the concave surface temperature remains constant at $T_i = 70°F(21°C)$ and the convex surface temperature increases.

The results presented Fig. 7a indicate that curved panels with negative Gaussian curvature have a monotonically increasing fundamental frequency, in general, as the concave surface temperature T_i increases. As the temperature increases, the panels deflect toward the positive x_3 direction into a deformed surface with higher negative curvature along the x_2 axis and lower positive curvature along the x_1 axis. The stiffness of the panel is increased by this type of deformation, which is amplified as the temperature increases. The increase in stiffness increases the fundamental frequency. The negative curvature becomes more dominant than the positive curvature as ℓ/R_2 becomes more negative, and the fundamental frequency increases with increasing negative curvature. A similar trend is shown in Fig. 7b for the panels with positive Gaussian curvature and $T_i = 70°F$ (21°C) and with an increasing convex-surface temperature.

The results presented in Fig. 7a also indicate that panels with nonnegative Gaussian curvature respond differently than panels with negative Gaussian curvature. Panels with $\ell/R_2 = 0$ and 0.01 have a limit-point instability response for values of temperature T_0 indicated by the filled symbols on the figure. For these cases, the panels deflect toward their projected planform and their bending stiffness is reduced, which reduces their fundamental frequencies. After buckling into the secondary stable equilibrium state, an increase in temperature generates a deformed panel with an increased positive Gaussian curvature. Increasing this curvature increases the panel bending stiffness, which increase the fundamental frequency. For values of $\ell/R_2 \geq 0.05$, the panels do not have a limit-point instability response. Similar trends are shown in Fig. 7b for panels with negative Gaussian curvature and $T_i = 70°F$ (21°C) and with an increasing convex-surface temperature.

The effects of panel curvature and an external transverse pressure load p_3 on the fundamental frequency of single-layer cylindrical panels with $\ell/h = 40$ and $E/G' = 30$ are shown in Fig. 8. The pressure p_3 is given by Eq. (3) with $m = n = 1$. Results for panels with nonnegative values of ℓ/R_2 up to 0.5 and subjected to a uniform temperature distribution with $T_i = T_e = 70°F$ (21°C) are shown in the figure. The results indicate that increasing the pressure load on flat panels increases the fundamental frequency of the panel. This increase in fundamental frequency is a result of an increase in the membrane stiffness of the panel due to stretching and an increase in the panel bending stiffness due to the out-of-plane deformation of the panel. This trend reverses as the panel curvature ℓ/R_2 increases. For this condition, increasing the external pressure load tends to flatten the panel and decreases the panel membrane and bending stiffnesses.

Results for Different Transverse-Shear-Deformation Theories

The effects of using different transverse-shear-deformation theories for predicting the interaction of the applied thermal load and the fundamental frequency of a panel are indicated by the results presented in Fig. 9 for three-layer panels with $\ell/h = 30$. The panels are subjected to an axial-compression prebuckling load that is 80% of the corresponding buckling load. Results are presented for the present HSDT, classical theory (CLT), and first-order transverse-shear-deformation theory (FSDT). The results are for flat panels with a uniform through-the-thickness temperature increase. The symbol k^2 shown in the figure corresponds to values of the shear correction factor used for the FSDT. Results are presented for values of $k^2 = \frac{2}{3}, \frac{5}{6}$, and $\pi^2/12$. The results indicate that all three theories predict the same general trends, but the values of the frequency predicted by CLT are significantly different from the values predicted by the transverse-shear-deformation theories. The HSDT and FSDT results agree very well for values of $k^2 = \frac{2}{3}$. The results presented in Refs. 12 and 13 indicate that the FSDT and HSDT results agree better with values of $k^2 = \frac{5}{6}$ for a single-layer panel. Results for cylindrical panels with $\ell/R_2 = 0.1$ and with a through-the-thickness temperature gradient with a constant value of $T_e = 70°F$ (21°C) are similar to the results shown in Fig. 4b with different values of E/G' and are presented in Ref. 23.

Concluding Remarks

The results of a parametric study of the vibration behavior of flat and shallow curved panels subjected to temperature fields and mechanical loads are presented. The mechanical loads include uniform axial-compression prebuckling loads and transverse-lateral pressure. The temperature fields include spatially nonuniform heating over the panel surfaces, and a linear through-the-thickness temperature gradient. The structural analysis used in the study is based on a HSDT of shallow shells that incorporates the effects of geometric nonlinearities and initial geometric imperfections. Analytical results are presented for simply supported single-layer and three-layer panels made from transversely isotropic materials. The results identify the interactions of the applied thermal and mechanical loads with the fundamental frequencies of the panels in both the prebuckling and postbuckling equilibrium states. The results indicate that a number of structural parameters and characteristics can significantly influence the response of a panel and should be considered in the design of flat and curved panels subjected to a thermal load. These parameters and characteristics include transverse-shear flexibility, initial geometric imperfections, temperature gradients, panel curvature, axial-compression prebuckling loads, and transverse lateral pressure. In general, the results indicate that the response and loading conditions that increase panel curvature increase the fundamental frequency, and those that decrease panel curvature decrease the fundamental frequency. Panels with initial or response-induced curvature can have a limit-point instability response for some through-the-thickness thermal gradients.

Acknowledgment

The work reported herein was partially supported by NASA Grant NAG1-1300.

References

[1]Bisplinghoff, R. L., and Pian, T. H. H., "On the Vibrations of Thermally Buckled Bars and Plates," *Proceedings of the 9th International Congress for Applied Mechanics* (Brussels), Vol. 7, 1957, pp. 307–318.

[2]Almroth, B. O., Bailie, J. A., and Stanley, G. M., "Vibration Analysis of Heated Plates," *AIAA Journal*, Vol. 15, No. 12, 1977, pp. 1691–1695.

[3]Yang, T. Y., and Han, A. D., "Buckled Plate Vibrations and Large Amplitude Vibrations Using High-Order Triangular Elements," *AIAA Journal*, Vol. 21, No. 5, 1983, pp. 758–766.

[4]Zhou, R. C., Xue, D. Y., Mei, C., and Gray, C. C., "Vibration of Thermal Buckled Composite Plates with Initial Deflections Using Triangular Elements," AIAA Paper 93-1321, April 1993.

[5]Lee, J., "Large Amplitude Plate Vibration in an Elevated Thermal Environment," U.S. Air Force Rept., WL-TR-92-3049, Wright–Patterson AFB, OH, June 1992.

[6]Murphy, K. D., Virgin, L. N., and Rizzi, S. A., "Free Vibration of Thermally Loaded Panels Including Initial Imperfections and Post-Buckling Effects," *Structural Dynamics: Recent Advances*, edited by N. S. Ferguson, H. F. Wolfe, and C. Mei, *Proceedings of the 5th International Conference*, Vol. 1, Inst. of Sound and Vibration Research, Univ. of Southampton, England, UK, 1994, pp. 401–411.

[7]Kornecki, A., "On the Thermal Buckling and Free Vibration of Cylindrical Panels Heated From Inside," *Bulletin of the Research Counsel of Israel*, Vol. 11C, No. 1, 1962, pp. 123–140.

[8]Tauchert, T. R., "Thermally Induced Flexure, Buckling and Vibration of Plates," *Applied Mechanics Review*, Vol. 44, No. 8, 1991, pp. 347–360.

[9]Noor, A. K., and Burton, W. S., "Computational Models for High-Temperature Multilayered Composite Plates and Shells," *Applied Mechanics Review*, Vol. 45, No. 10, 1992, pp. 414–446.

[10]Librescu, L., Lin, W., Nemeth, M. P., and Starnes, J. H., Jr., "Vibration of Geometrically Imperfect Laminated Flat and Shallow Curved Panels Subjected to Heating and a System of Mechanical Loadings," *Proceedings of the 10th DoD/NASA/FAA Conference on Fibrous, Composites and Structural Design* (Hilton Head, SC), Naval Air Warfare Center Rept., NAWCADWAR-94096-60, Vol. 2, 1994, pp. IX-51–IX-66.

[11]Librescu, L., and Chang, M.-Y., "Effects of Geometric Imperfections on Vibration of Compressed Shear Deformable Laminated Composite Curved Panels," *Acta Mechanica*, Vol. 96, Nos. 1–4, 1993, pp. 203–224.

[12]Librescu, L., and Chang, M.-Y., "Vibration of Compressively Loaded Shear Deformable Flat Panels Exhibiting Initial Geometric Imperfections," *AIAA Journal*, Vol. 30, No. 11, 1992, pp. 2793–2795.

[13]Librescu, L., and Chang, M.-Y., "Imperfection Sensitivity and Postbuckling Behavior of Shear-Deformable Composite Doubly-Curved Shallow Panels," *International Journal of Solids and Structures*, Vol. 29, No. 9, 1992, pp. 1065–1083.

[14]Librescu, L., Chandiramani, N. K., Nemeth, M. P., and Starnes, J. H., Jr., "Postbuckling of Laminated Flat and Curved Panels Under Combined Thermal and Mechanical Loadings," AIAA Paper 93–1563, April 1993.

[15]Librescu, L., Lin, W., Nemeth, M. P., and Starnes, J. H., Jr., "Classical Versus Non-Classical Postbuckling Behavior of Laminated Composite Panels Under Complex Loading Conditions," *Non-Classical Problems of the Theory and Behavior of Structures Exposed to Complex Environmental Conditions*, AMD-Vol. 164, Applied Mechanics Div., American Society of Mechanical Engineers, New York, 1993, pp. 169–182.

[16]Librescu, L., *Elasto-Statics and Kinetics of Anisotropic and Heterogeneous Shell-Type Structures*, Noordhoff International, Leyden, The Netherlands, 1975.

[17]Terner, E., "On Thermal Stresses in Certain Transversely Isotropic, Pyrolitic Materials," *Proceedings of the Fourth U.S. National Congress of Applied Mechanics*, American Society of Mechanical Engineers, New York, 1962, pp. 1147–1152.

[18]Seide, P., "A Reexamination of Koiter's Theory of Initial Postbuckling Behavior and Imperfection Sensitivity of Structures," *Thin Shell Structures: Theory, Experiment and Design*, edited by Y. C. Fung and E. E. Sechler, Prentice–Hall, Englewood Cliffs, NJ, 1974, pp. 59–80.

[19]Ilanko, S., and Dickinson, S. M., "The Vibration and Post-Buckling of Geometrically Imperfect, Simply Supported Rectangular Plates under Uni-Axial Loading, Part II. Experimental Investigation," *Journal of Sound and Vibration*, Vol. 118, No. 2, 1987, pp. 337–351.

[20]Hui, D., and Leissa, A. W., "Effects of Geometric Imperfections on Vibrations of Biaxially Compressed Rectangular Plates," *Journal of Applied Mechanics*, Vol. 50, No. 4, 1983, pp. 750–756.

[21]Kapania, R. K., and Yang, T. Y., "Buckling, Postbuckling and Nonlinear Vibrations of Imperfect Plates," *AIAA Journal*, Vol. 25, No. 10, 1987, pp. 1338–1346.

[22]Heinen, J. W., "Vibration of Geometrically Imperfect Beam and Shell Structures," *International Journal of Solids and Structures*, Vol. 27, No. 1, 1991, pp. 29–47.

[23]Librescu, L., Lin, W., Nemeth, M. P., and Starnes, J. H., Jr., "Effects of a Thermal Field on the Frequency-Load Interaction of Geometrically Imperfect Shallow Curved Panels," AIAA Paper 94-1342, April 1994.